Prediction of Residual Stresses of 3d-Printed Plates Utilizing SYSWELD

Abdulrahman A. Alrumayh

Department of Mechanical Engineering, College of Engineering, Qassim University, Buraydah 51452, Saudi Arabia. Email: A.Alrumayh@qu.edu.sa

H. F. Nied

Mechanical Engineering and Mechanics, Lehigh University, Bethlehem, PA 18015, USA, email: hfn2@lehigh.edu

Abdulaziz A. Alrumayh

Drilling and Workover, Saudi Arabian Oil Company, Dhahran, 31311, Saudi Arabia, Email: Abdulaziz.Alrumayh@aramco.com

A. E. Abdelraheim

Department of Mechanical Engineering, College of Engineering, Qassim University, Buraydah 51452, Saudi Arabia. Email: aahmad@qu.edu.sa

[Received: 5 March 2025, Revised: 26 March 2025, Accepted: 26 March 2025, Published 11 May 2025]

Abstract: Investigating how residual stress distribution evolves with increasing build height (number of layers) is crucial for understanding scalability and dimensional control in additive manufacturing. Post-processing, such as unclamping, machining, and heat treatment, interacts with the existing stress state and influences varying build heights (number of layers). This was the subject of speculation of many up-to-date researchers. Among the drawbacks of the residual stress is its impact on fatigue crack propagation. This work investigates the residual stress prediction in 3D-printed plates using the SYSWELD simulation software. The investigation covers the evolved residual stress after finishing each of the manufacturing phase. It focuses on the Wire Arc Additive Manufacturing (WAAM) process, a widely used metal 3D-printing technique. The SYSWELD finite element software was utilized for predicting the residual stress after clamping, unclamping, surface finishing and heat treatment. The study aims to improve simulation accuracy by incorporating a round-layer design model, which better represents the actual deposition process compared to traditional layer-based approaches. Fourteen sets of results for different numbers of layers, ranging from 5 layers to 150 layers. The use of SYSWELD facilitate modeling the thermal and mechanical behavior of the printed plates, incorporating factors such as heat input, material properties, and cooling effects. The study ends with providing a way of predicting the expected residual stress after each process of additive manufacturing.

Keywords: Additive Manufacturing; WAAM; Residual Stresses; Heat Treatment; Size Effects.

1. INTRODUCTION

Wire Arc Additive Manufacturing (WAAM) is well known for its high deposition and ability to produce large parts, but it suffers from challenges like high residual stresses. These residual stresses can lead to dimensional inaccuracies and distortion, which may require further processing. Understanding and predicting these residual stresses is crucial to optimizing WAAM's effectiveness and reducing post-processing costs [1 and most of its references].

In thin-walled parts; if the large residual stresses created by the WAAM processes was not relieved, this, can lead to undesirable distortion [2]. Since WAAM is based on well-understood direct fusion welding processes, conventional welding process parameters can be effectively utilized and controlled with little trial and error. The most crucial welding parameters are the arc voltage, arc current, shielding gas, nozzle-base distance, travel speed, wire feed speed, and wire diameter. Venturini, F. et al concluded in [3] that the resulting residual stresses, the weld bead geometry, and the distortion, are strongly influenced by the previously stated process parameters. Similar to other fusion welding techniques, Wire Arc Additive Manufacturing (WAAM) commonly faces challenges such as incomplete fusion,

porosity, vaporization, undesirable heat-affected zone properties, grain structure issues, poor surface finish, deformation and distortion, high residual stresses, and cracking [4].

Fortunately, post-weld heat treatment can alleviate some of these issues stemming from reversible thermal effects. A frequently controllable problem is the weld bead profile quality, which is mainly affected by layer thickness variations, undercutting, and asymmetrical beads [5-6]. Residual stresses in WAAM can lead to work piece distortion or cracking. The sequential heating and cooling of deposited layers during the AM process create complex thermal cycles [7]. As a high heat input process, WAAM can produce a large heat-affected zone, potentially causing undesirable metallurgical changes and localized cracking. Significant residual stresses can develop with large thermal gradients and high work piece constraint. While unclamping can offer some stress relief, it may also cause war page. Notably, the highest residual stress component often aligns with the deposition path [6].

The formation of residual stress in WAAM is influenced by factors like the number of layers, deposition strategies, and substrate thickness [8-9], as well as temperature and travel speed, highlighting the importance of optimization and simulation for minimizing and predicting stress buildup [10-11]. Various methods, including substrate preheating, selective secondary heating, weld path optimization, and high-pressure rolling, have been explored to improve build geometry, residual stresses, and metallurgical properties in WAAM [12]. Given the numerous controllable welding parameters, relying solely on experimentation for process optimization is inefficient. Computational simulations are recognized as valuable tools for developing improved WAAM processes based on established welding physics.

Non-destructive tests are considered ways to measure and analyze residual stresses. However, they have some limitations, such as the temperature and the wavy surfaces [13]. This explains why numerical simulations, particularly those using software like SYSWELD, are vital tools for predicting residual stresses in WAAM. Finite Element Modeling (FEM) is considered as a reliable and essential tool for understanding and predicting stress behavior during deposition and post-processing [11,14].

While simulation methods advance, challenges remain, particularly in simulating complex geometries and optimizing process parameters. A simplified representation of the predicted residual stress during and after the printing process is vital for the industry to advance.

Simulating the transient heat transfer and residual stress evolution in welding processes is best accomplished using finite element analysis (FEA) codes due to the highly nonlinear thermomechanical behavior involved. Although general-purpose commercial software can be applied to welding simulations, it may be inefficient for modeling specific processes. This study utilized ESI's specialized FEA welding simulation software, SYSWELD [15], which provides integrated tools to easily input welding parameters that can be adequately described by a predefined moving heat source [16]. SYSWELD also allows for the prediction of phase proportions, hardness, distortions, residual stresses, and plastic strain distributions after heat treatment [17]. For a thorough understanding and improvement of the WAAM process, detailed simulation of multi-pass welding with varied deposition paths and parameters is desirable. However, a direct, layer-by-layer modeling approach for complex AM builds is computationally impractical with current capabilities. While simulating a limited number of weld passes (up to a few hundred) is feasible, the detailed information from these localized models can be leveraged to develop more efficient global simulation models. These global models would be built upon

the local models, integrating local temperatures, stresses, and strains into a broader simulation framework.

2. SYSWELD MODEL

Most of the reviewed papers [1-17] use a square-layer design model in their studies. The square layer design model lacks the ability to show some of the stress concentration areas that are generated during and after the manufacturing process. This was the reason for developing the SYSWELD model in this work—to simulate a round-layer design, which results in a more realistic representation of residual stresses. Figure 1 shows the difference between the model with a round layer design and the square layer design. The colored-scale to the right gives stress in MPa.

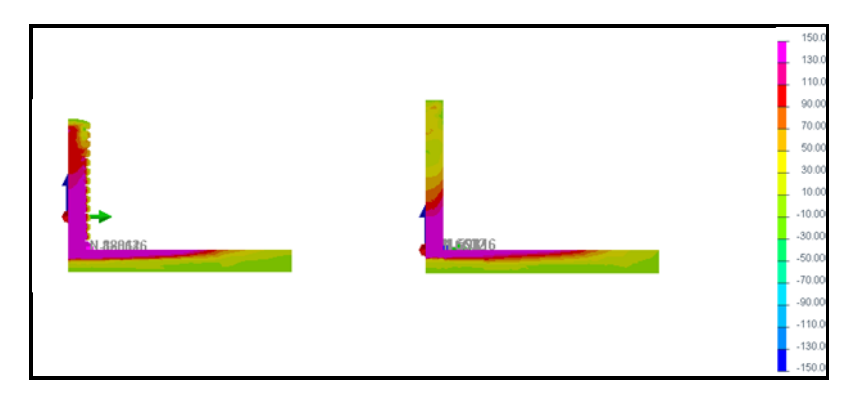


Figure 1: Round Layer (Left) versus Square Layer (Right).

3. RESULTS AND DISCUSSION

Both the First Principal Stress (FPS) and the XX-stresses are interesting. This was studied for each specimen in the front view (FV) and at the cross-sectional area (CS). Four sets of results may be obtained for each specific number of layers. Two approaches may be followed in the results analysis and discussion: (1) the first approach is to study and analyze the obtained results (study the stress change) for a specific number of layers in the four phases (Clamped, Unclamped, Machined, and Heat-Treated). The other approach, however, (2) is to study several cases of the number of layers for the same phase.

1. Study and analyze the results for the case of 30 layers in the four phases: The residual stress distribution for the four sets (FPS&FV, FPS&CS, XX&FV and XX&CS) are given in Figure 2. The left result column consists of 4 pictures representing the clamped case's stress distribution. Studying this result column may indicate that both FPS and XX stresses represent high tension ≈ +150 MPa on the uppermost and lowermost layers of the printed part, including the base. This is done by excluding the ends of the upper layers, which turned out to be neutral (-10 to -20 MPa). The central area is on high compression for XX ≈-150MPa and neutral (-10 to -20 MPa) for FPS, which aligns with the observation recorded by Alrumayh et a. [1]. In the next column, the stresses are slightly relieved for the unclamped phase. These stresses continued to be relieved from the second column (unclamped) to the third column (machined) and reached their most relieved state after heat treatment. Additional high XX compression zones form on the surface of the far ends of the central layers. Additionally, the XX compression on the base's surface gradually decreases.

It is also clear that, for all cases, the stress distribution differs as the normal distance to the base increases.

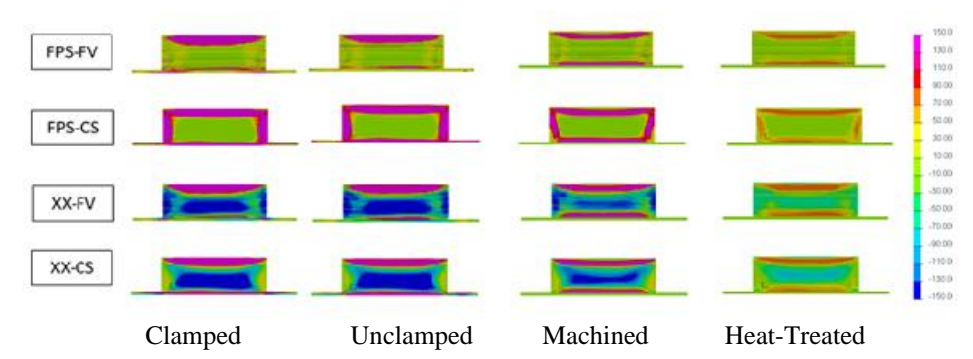


Figure 2: The residual stress distribution for (Clamped, Unclamped, Machined, and Heat-Treated) - case of 30 Layers

2. Study cases of 30, 40, 50, and 60 layers at the clamped phase only. The residual stress distribution for the four sets (FPS&FV, FPS&CS, XX&FV, and XX&CS) is given in Figure 3.

Figure 3 represents the effect of the number of layers on the four types of residual stresses for the clamped case. The left result column is for the 30-layer-case, following three columns, however, are for 40, 50, and 60 layers, respectively. It is clear now that the distribution of the stresses spreads widely as the number of layers increases.

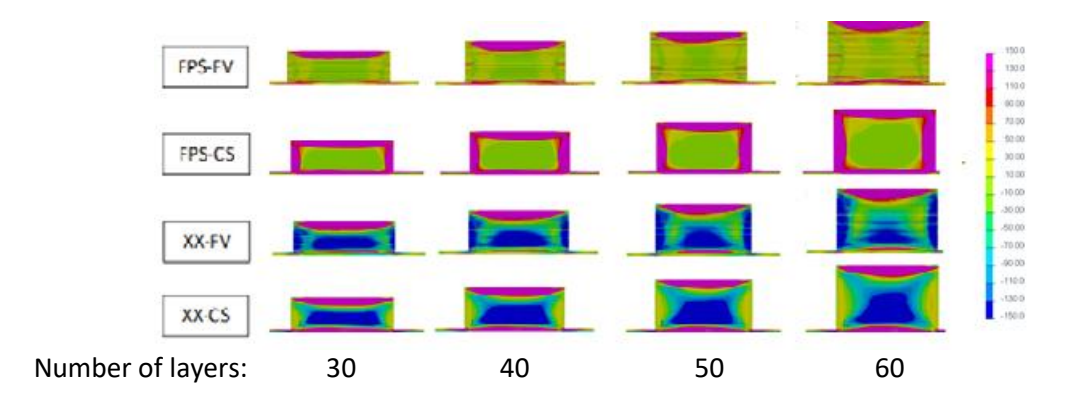


Figure 3: The effect of the number of layers on the four types of residual stresses considering the clamped case

4. STUDY THE EFFECT OF THE NUMBER OF LAYERS AND THE DISTANCE FROM THE BASE ON THE STRESS DISTRIBUTION

The effect of the number of layers on the change of the stress distribution was studied for the cases of 5 layers to 150 layers. The distance from the base of the middle plane was selected to record the stresses. The distance was normalized in terms of the total specimen depth. In addition, the number of layers is normalized by 10. In this sense, the following parametric study provides the stress magnitude at a certain point on the middle plane for each selected number of layers. The results are summarized in eight figures. These eight figures are given in Figure 4 (a, b, c and d) and Figure 5 (a, b, c and d). Figure 4 is

used to study the XX-stress, while Figure 5 is utilized to study the FP-stress. Full description for these figures is given in Table 1:

Table 1 Full description for the XX-stress investigation cases:

		Clamped	Unclamped	Machined	Heat treated
XX		1	2	3	4
	Figure 4	а	b	С	d
FPS		5	6	7	8
	Figure 5	а	b	С	d

5. DISTRIBUTIONS OF THE XX-STRESS

In general, the four figures show that the stress distribution starts in tension at the top and bottom points with almost the same tension value for the same number of layers. The stress decreased and switched to compression stress as the NDR increased till around 60% where it reached its maximum compression value.

Fig. 4-a gives the distribution of the stresses on a point on the middle plane with a normalized distance (NDR) from the base for several layers from 5 to 150 for the clamped case. Investigating Fig. 4-a may lead to the summary given in Table 2:

Table 2 Change in stress on a point on the middle plane for the <u>clamped</u> cases:

NDR	Stress behavior as the number of layer	Change in stress MPa	
NDK	increases	From	То
Around 10%:	Slightly decreases	320	300
10% <ndr<90%< td=""><td>Decreases</td><td>+300</td><td>-120</td></ndr<90%<>	Decreases	+300	-120
90% <ndr< td=""><td>Increases</td><td>200</td><td>320</td></ndr<>	Increases	200	320

Fig. 4-b and c give the distribution of the stresses on a point on the middle plane with a normalized distance (NDR) from the base for several layers from 5 to 150 for the Unclamped and the machining cases. Table 3 describes the distribution as:

Table 3 Change in stress on a point on the middle plane for the <u>Unclamped and the machining</u> cases:

NDR	Stress behavior as the number of layer	Change in stress MPa	
NDK	increases	From	То
Around 10%:	Slightly decreases	320	300
Around 60%:	Decreases (from 5 to 70 layers)	0	-250
Around 60%:	Increases (from 70 to 150 layers)	-250	-120

Fig. 4-d gives the distribution of the stresses on a point on the middle plane with a normalized distance (NDR) from the base for several layers from 5 to 150 for the heat-treated cases. Investigating the figure shows the changes summarized in Table 4:

Table 4 Change in stress on a point on the middle plane for the <u>heat-treated</u> cases:

NDR	Stress behavior as the number of layer	Change in stress MPa	
	increases	From	То
Around 10%:	Slightly increases	40	70
Around 60%:	Decreases (from 5 to 70 layers)	0	-120
Around 60%:	Increases (from 70 to 150 layers)	-120	-45

It is clear now that the heat treatment decreases the amount of residual stress in both the tension and compression cases.

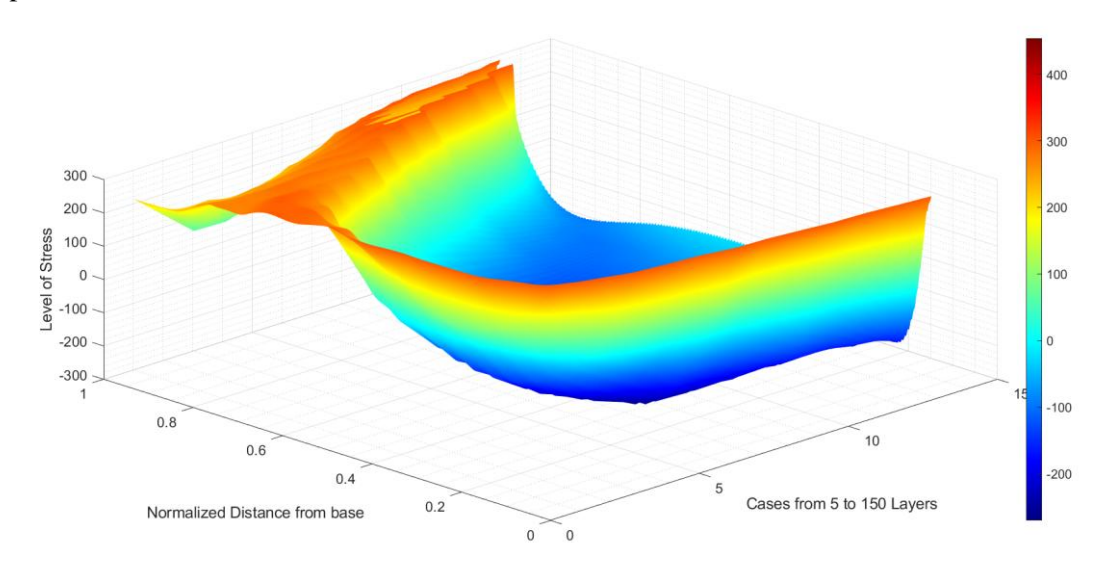


Figure (4-a) Distribution of XX-stresses for the clamped case

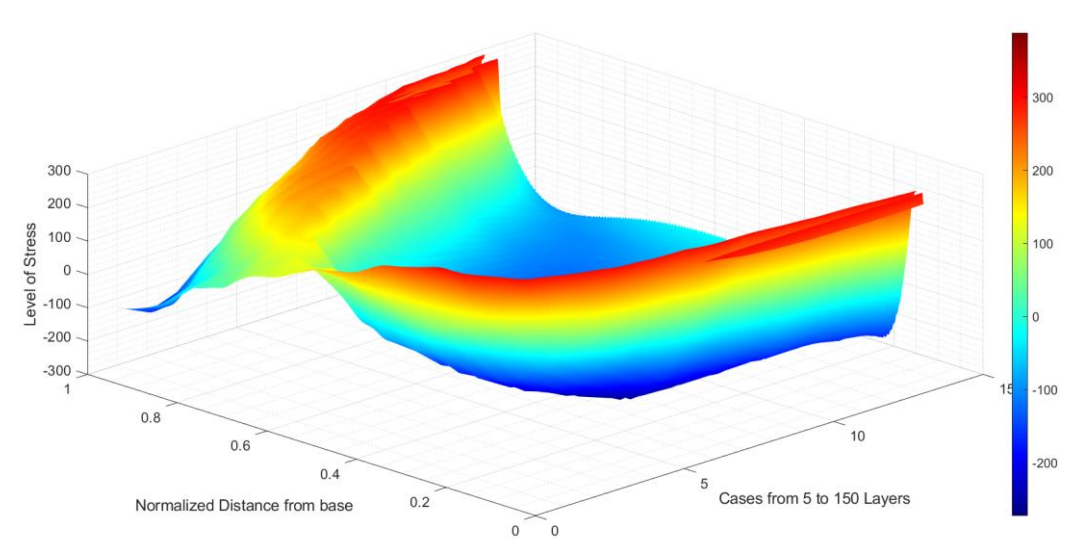


Figure (4-b) Distribution of XX-stresses for the Un-clamped case

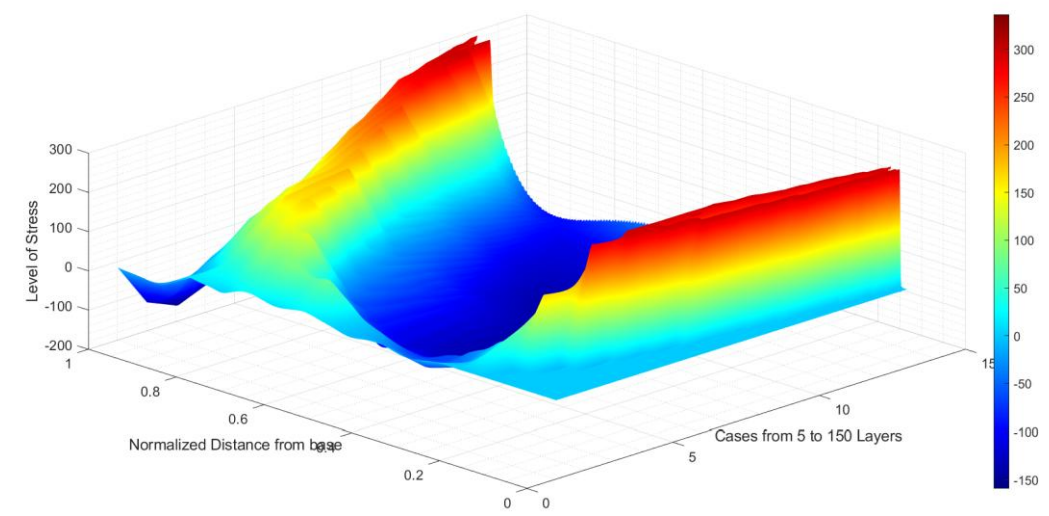


Figure (4-c) Distribution of XX-stresses for the machined case

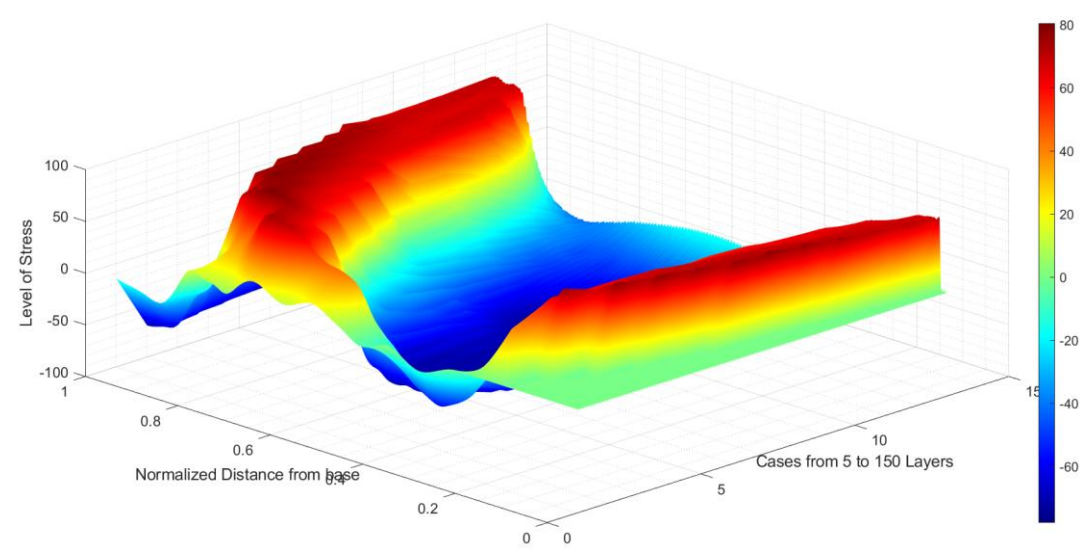


Figure (4-d) Distribution of XX-stresses for the heat treated case

6. DISTRIBUTIONS OF THE FIRST PRINCIPAL STRESS

In general, the four figures show that the stress distribution starts in tension at the top and bottom points with almost the same tension value for the same number of layers. The stress decreased and switched to compression stress as the NDR increased till around 50% where it reaches its maximum compression value. The distribution of the FPS shows that the region for maximum FPS sherinked compared with that of the XX-stress distribution.

Fig. 5-a gives the distribution of the stresses on a point on the middle plane with a normalized distance (NDR) from the base, for cases of several layers from 5 to 150, for the clamped case. Investigating the figure shows that:

For NDR \leq 10% and NDR \geq 90%, the stress is almost 320MPa.In between, the stresses decreases until it touches no stress at almost 40%, then increases again. The two highest values at the bottom and top occur for all the layers but with different values. For low number of layers, the stress almost does not exist. At the highest number of layers, however, it reaches the maximum of 320 MPa. The minimum value of stresses may be found for all layers of the NDR between 35 and 75%.

The stress distribution profile for the unclamped case given in Fig. 5-b is almost the same as that of the clamped case. The main difference between both cases is that the maximum stress (320MPa) may be found only for cases where the number of layers exceeds 110.

The stress distribution profile for the machined and the heat-treated cases given in Fig. 5-c and 5-d is almost the same as that of the unclamped case. The main difference between both cases is that at this case the maximum stress (400MPa) at the base and 300MPa at the top may be found only for the cases of NDR<number of layers exceeds 110 layers.

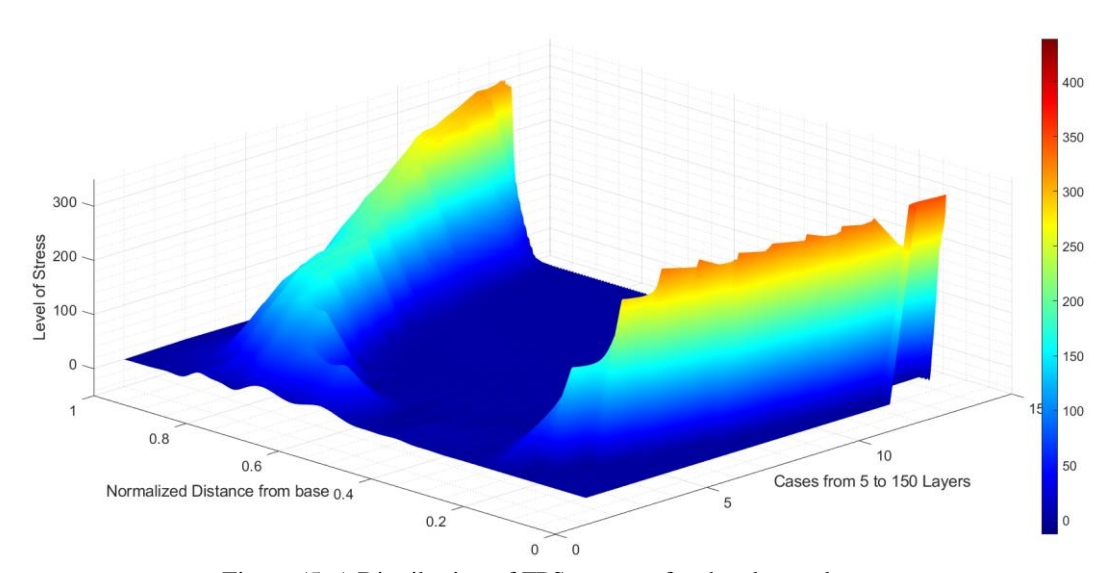


Figure (5-a) Distribution of FPS-stresses for the clamped case

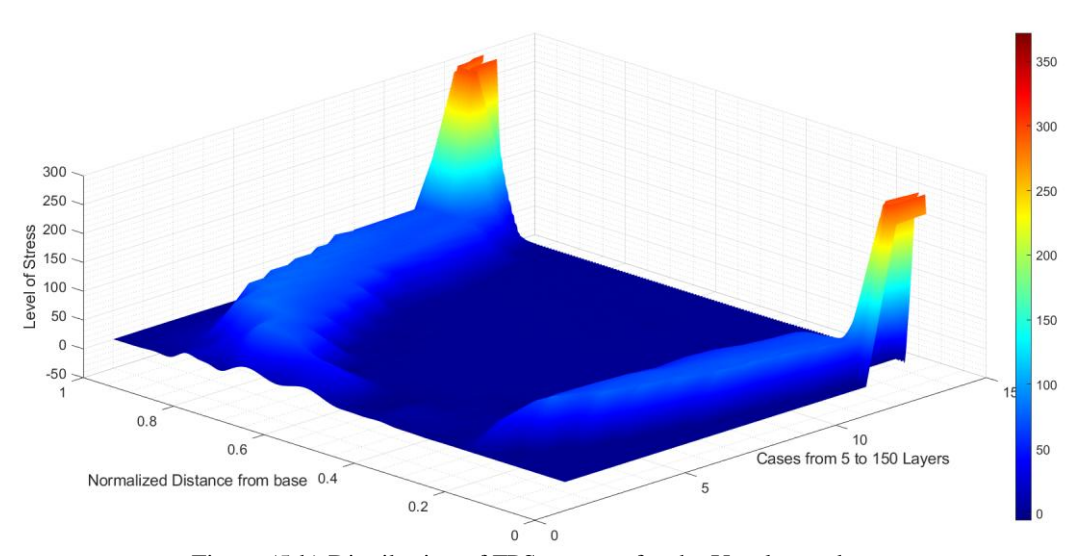


Figure (5-b) Distribution of FPS-stresses for the Un-clamped case

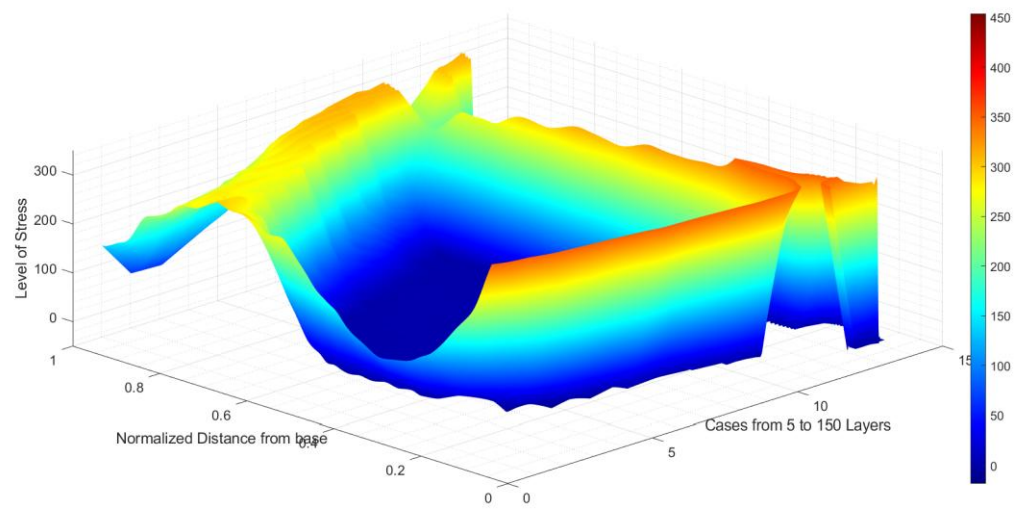


Figure (5-c) Distribution of FPS-stresses for the machined case

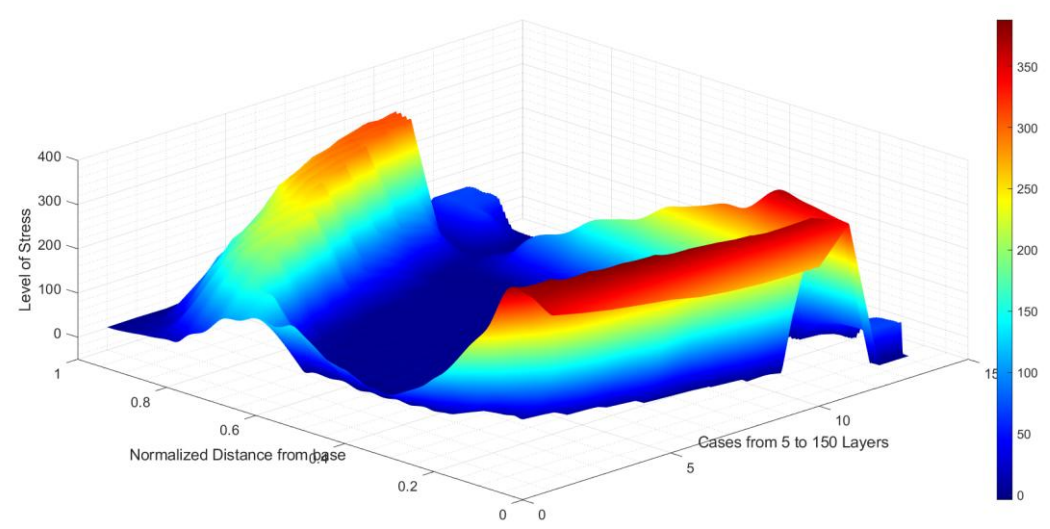


Figure (5-d) Distribution of FPS-stresses for the heat-treated case

7. 7SUMMARY AND CONCLUSIONS

The residual stresses on the WAAM printed parts were simulated and summarized in eight contour graphs, each representing a set of cases. The data for these graphs were acquired using the commercially available software SYSWELD, which utilized finite element analysis. The simulation was executed in austenitic stainless-steel grade 316L. The following points may summarize the conclusions:

- 1. As expected, both First Principal Stress and XX Stress generated during the printing process significantly change as the number of layers increases. The most drastic changes occur during the first 40–60 layers. After that, the rate of change starts to decrease. Moreover, the effect of post-printing conditions on these stresses is limited, and the most significant change occurs after heat treatment.
- 2. The proposed round-layer model provides more realistic stress distribution predictions.
- 3. Residual stresses vary across different plate regions, with higher tensile stresses near the top layers and compressive stresses in lower layers.
- 4. The results align well with existing experimental trends, demonstrating the effectiveness of the improved modeling approach.

In future work; the authors recommend doing more research to investigate the effect of layers, substrate geometry, and changes in the tested materials. In addition to performing more tests on the effect of different WAAM parameters and carrying out experimental validation

REFERENCES

- [1]- Alrumayh, Abdulrahamn & Nied, H.. (2024). SIMULATION OF RESIDUAL STRESSES DURING THE WIRE ARC ADDITIVE MANUFACTURING (WAAM) PROCESS. 10.3217/978-3-85125-968-1-15.
- [2]- H. GENG, J. XIONG, D. HUANG, X. LIN, J. LI(2017). A prediction model of layer geometrical size in wire and arc additive manufacture using response surface methodology, Int. J. Adv. Manuf. Technol, 93, pp. 175-186, 2017, doi:10.1007/s00170-015-8147-2.
- [3]- VENTURINI, F. MONTEVECCHI, A. SCIPPA, G. CAMPATELLI. (2016). Optimization of WAAM Deposition Patterns for T-crossing Features, Procedia CIRP, 55, 95-100, 2016, doi:10.1016/j.procir.2016.08.043.
- [4]- B.A. SZOST, S. TERZI, F. MARTINA, D. BOISSELIER, A. PRYTULIAK, T. PIRLING, M. HOFMANN, D.J. JARVIS (2016). A comparative study of additive manufacturing techniques: Residual stress and microstructural analysis of CLAD and WAAM printed Ti-6Al-4V components, Mater. Des, 89, pp. 559-567, 2016, doi: 10.1016/j. matdes.2015.09.115.
- [5]-A. BUSACHI, J. ERKOYUNCU, P. COLEGROVE, F. MARTINA, J. DING. (2015). Designing a WAAM based manufacturing system for defence applications, Procedia CIRP, 37, pp. 48-53, 2015, doi:10.1016/j.procir.2015.08.085.
- [6]- S.W. WILLIAMS, F. MARTINA, A.C. ADDISON, J. DING, G. PARDAL, P. COLEGROVE: 'Wire + Arc Additive Manufacturing, Mater. Sci. Technol, 32, pp. 641-647, 2016, doi:10.1179/1743284715Y.0000000073.
- [7]- J.Y. BAI, C.L. YANG, S.B. LIN, B.L. DONG, C.L. FAN. (2016). Mechanical properties of 2219-Al components produced by additive manufacturing with TIG, Int. J. Adv. Manuf. Technol, 86, pp. 479-485, 2016, doi:10.1007/s00170-015-8168-x.
- [8]- Derekar, Karan & Ahmad, Bilal & Zhang, Xiang & Joshi, Sameehan & Lawrence, Jonathan & Xu, Lei & Addison, Adrian & Melton, Geoff. (2021). EFFECTS OF PROCESS VARIANTS ON RESIDUAL STRESSES IN WIRE ARC ADDITIVE MANUFACTURING OF ALUMINUM ALLOY 5183. Journal of Manufacturing Science and Engineering. 144. 1-35. 10.1115/1.4052930.
- [9]- Sun, Jiamin & Hensel, Jonas & Köhler, Markus & Dilger, Klaus. (2021). RESIDUAL STRESS IN WIRE AND ARC ADDITIVELY MANUFACTURED ALUMINUM COMPONENTS. Journal of Manufacturing Processes. 65. 97-111. 10.1016/j.jmapro. 2021.02.021.
- [10]- Gurmesa, Fakada & Lemu, Hirpa & Wakjira, Yosef & Harsibo, Mesfin. (2024). RESIDUAL STRESSES IN WIRE ARC ADDITIVE MANUFACTURING PRODUCTS AND THEIR MEASUREMENT TECHNIQUES: A SYSTEMATIC REVIEW. Applied Mechanics. 5. 420-449. 10.3390/applmech5030025.
- [11]- Feng, Guangjie & Wang, Hu & Wang, Yifeng & Deng, Dean & Zhang, Jian. (2022). NUMERICAL SIMULATION OF RESIDUAL STRESS AND DEFORMATION IN WIRE ARC ADDITIVE MANUFACTURING. Crystals. 12. 803. 10.3390/cryst 12060803.
- [12]- S. SURYAKUMAR, K.P. KARUNAKARAN, U. CHANDRASEKHAR, M.A. SOMASHEKARA. (2013). A study of the mechanical properties of objects built through weld-deposition, Proc. Inst. Mech. Eng., Part B: J. Eng. Manuf., 227(8), pp. 1138-1147, 2013, doi:10.1177/0954405413482122.
- [13]- Rodrigues, Tiago & Duarte, Valdemar & Miranda, R.M. & Santos, Telmo & Oliveira, J. P.. (2019). CURRENT STATUS AND PERSPECTIVES ON WIRE AND ARC ADDITIVE MANUFACTURING (WAAM). Materials. 12. 1121. 10.3390/ma12071121.

- [14]- Montevecchi, Filippo & Venturini, Giuseppe & Scippa, Antonio & Campatelli, Gianni. (2016). FINITE ELEMENT MODELLING OF WIRE-ARC-ADDITIVE-MANUFACTURING PROCESS. Procedia CIRP. 55. 109-114. 10.1016/j.procir. 2016.08.024.
- [15]- SYSWELD 2021.0 Documentation Package, ESI North America, Farmington Hills, MI.
- [16]- W. WORLD, L.E. SOUDAGE, D. LE, T. GUWAHATI, T. BOMBAY. (2013). Efficient estimation of volumetric heat source in fusion welding process simulation, in Fusion Welding Process Simulation, 56, pp. 88-97, 2013, doi:10.1007/BF03321399.
- [17]- T. KIK, M. SLOVACEK, J. MORAVEC, M. VANEK. (2015). Numerical Simulations of Heat Treatment Processes, Appl. Mech. Mater, Trans Tech Publications, Vol. 809-810, pp. 799-804, 2015, doi:10.4028/www.scientific.net/AMM.809-810.799.

التنبؤ بالإجهادات المتبقية للالواح المطبوعة ثلاثية الأبعاد باستخدام SYSWELD

الملخص: يُعد التحقق من كيفية تطور توزيع الإجهاد المتبقي مع زيادة ارتفاع البناء (عدد الطبقات) أمرًا بالغ الأهمية؛ حيث يساعد ذلك في فهم قابلية التوسع والتحكم في الأبعاد في التصنيع بالإضافة. تتفاعل عمليات ما بعد المعالجة (مثل فك التثبيت والتشغيل والمعالجات الحرارية) مع حالة الإجهاد الموجودة وتؤثر على ارتفاعات البناء المختلفة للألواح (عدد الطبقات). وجدير بالذكر؛ أن هذا الموضوع كان محل إهتمام العديد من الأبحاث العلمية الحديثة المرتبطة بهذا المجال. ويعد تأثير الإجهاد المتبقى على إنتشار التشققات التي تطرأ نتيجة الكلل من اهم التأثيرات الضارة للإجهاد المتبقى.

يستخدم هذا العمل برنامج المحاكاة SYSWELD لحساب الإجهاد المتبقي في الألواح المنتجة بنظام الطباعة ثلاثي الأبعاد. كما تغطي هذه الحسابات الإجهاد المتبقي المتطور بعد الانتهاء من كل مرحلة من مراحل التصنيع. ويركز البحث على عملية التصنيع بالاضافة عبر استخدام القوس الكهربائي والسلك المعدني (WAAM) والتي تعد من أوسع تقنيات الطباعة ثلاثية الأبعاد للمعادن إنتشاراً. وقد تناول البحث مواضيع التنبؤ بالإجهاد المتبقي بعد التثبيت، وبعد فك التثبيت، و بعد از الة الاجزاء الزائدة بعملية التشغيل، وبعد المعالجة الحرارية.

ولتحسين دقة المحاكاة ذهبت الدراسة إلى إستخدام نموذج تصميم طبقة مستديره مشابه للواقع، وذلك لما يوفره من تمثيل لعملية البناء الفعلية بشكل أفضل إذا ما قورن بالطرق التقليدية في المحاكات القائمة على الطبقات المستطيلة. إشتمات الدراسة على أربعة عشر مجموعة من النتائج لأعداد مختلفة من الطبقات، تتراوح من 5 طبقات إلى 150 طبقة. وقد تم توظيف برنامج SYSWELD لنمذجة السلوك الحراري والميكانيكي للألواح المطبوعة، مع الأخذ في الإعتبار لعوامل مثل مدخلات الحرارة وخصائص المواد وتأثيرات التبريد. تختتم الدراسة بتقديم طريقة للتنبؤ بالإجهاد المتبقي المتوقع بعد كل عملية من عمليات التصنيع بالإضافة.